



UNIKLINIK
KÖLN

Zentrum für
Neurochirurgie

Klinik für Stereotaxie und funktionelle Neurochirurgie



Institut für Neurowissenschaften und Medizin



MR-Radiomics in Neuro-Oncology

M. Kocher

Klinik für funktionelle Neurochirurgie und Stereotaxie
Forschungszentrum Jülich, INM 4

29.5.2018 Hamburg | AK Computer und IMRT

Genomics

Applications for Neuro-Oncology

Gene Mutation Patterns

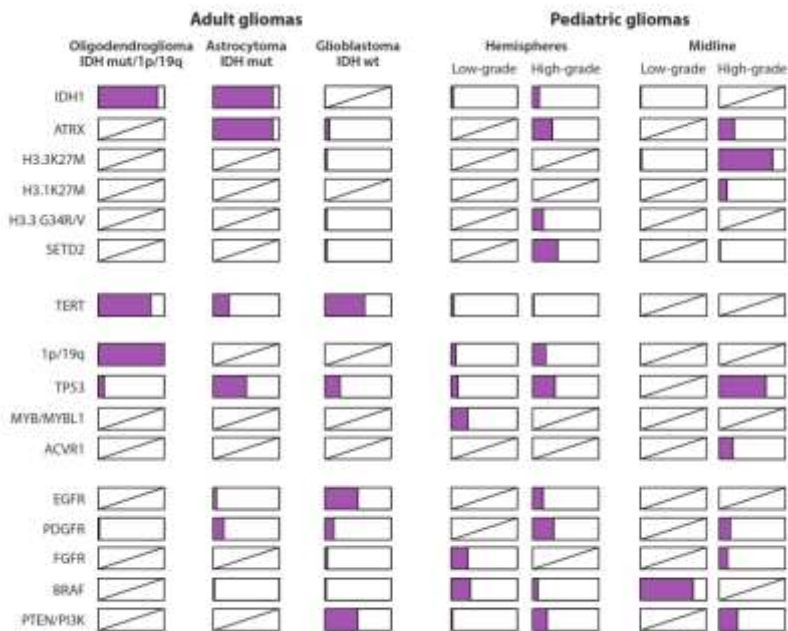


Figure 1
Genomic alterations in pediatric and adult gliomas. Recurrently mutated genes in pediatric and adult gliomas. Size of the colored bar represents the average percentage of cases with a specific mutation. Abbreviations: mut, mutated; wt, wild-type.

Gene Expression (mRNA)

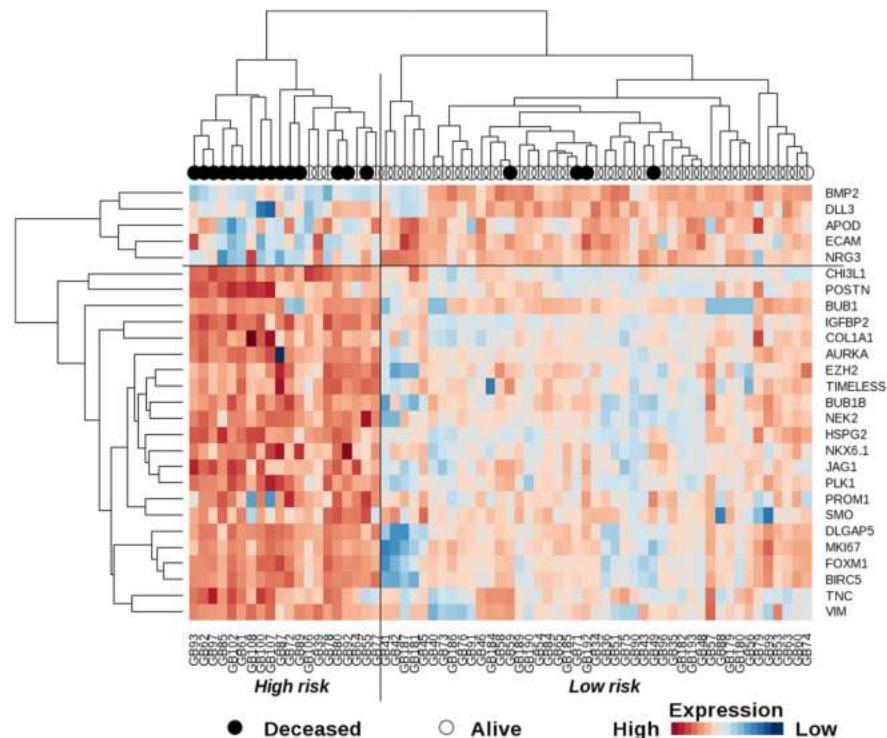


Figure 1. Gene expression heatmap and overall survival of WHO grade II/III glioma patients. Map of the gene expression levels from the 27-gene list used to generate a classification clearly identifying a high risk cluster containing most of the deceased patients of the training cohort. doi:10.1371/journal.pone.0066574.g001

Radiomics: Feature description

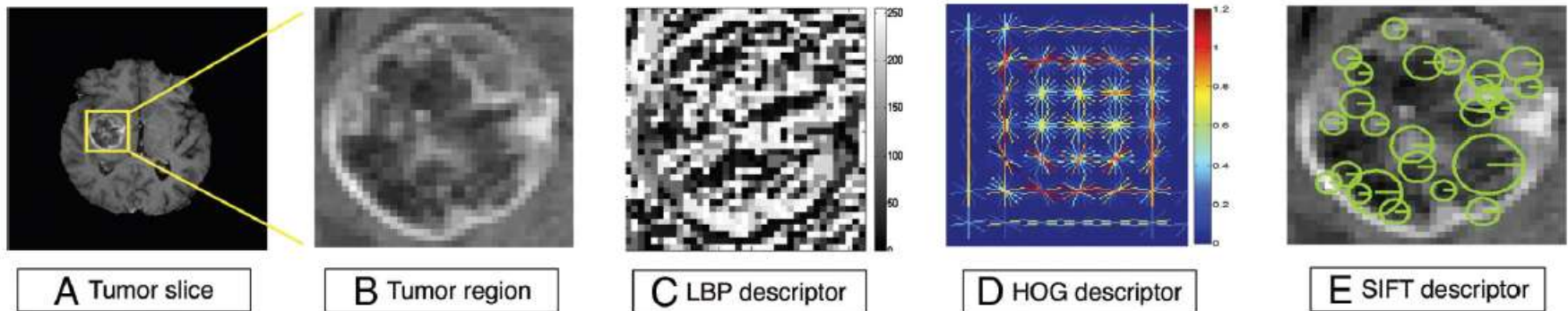


FIG 1. Visualization of computational image feature descriptors. A T1-weighted brain tumor section (A and B) is displayed, and feature visualizations (C–E) are given of LBP (C), HOG (D), and SIFT (E) descriptors. LBP quantifies local pixel structures through a binary coding scheme. HOG computes block-wise histogram gradients with multiple orientations. SIFT detects distributed key points with radius on tumor images. These multiparametric features create a rich image-driven data base to characterize tumors in MR imaging at different scales.

LBP: Local Binary Patterns
HOG: Histogram of Oriented Gradients
SIFT: Scale Invariant Feature Transform

Radiomics in Brain Tumor: Image Assessment, Quantitative Feature Descriptors, and Machine-Learning Approaches

M. Zhou, J. Scott, B. Chaudhury, L. Hall, D. Goldgof, K.W. Yeom, M. Iv, Y. Ou, J. Kalpathy-Cramer, S. Napel, R. Gillies, O. Gevaert, and R. Gatenby

Radiomics

Applications for Neuro-Oncology

Microscopical and molecular tumor characteristics :

- Cell type
- Receptor expression
- Invasion pattern
- Angiogenesis
- Gene mutations

TISSUE + PATHOLOGIST

Can be assessed
using imaging methods

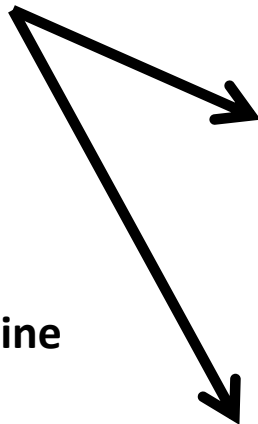


Radiomics :

- General tumor features:
 - Histogram
 - Texture
 - Shape
- Local image feature maps

IMAGES + SOFTWARE

determine

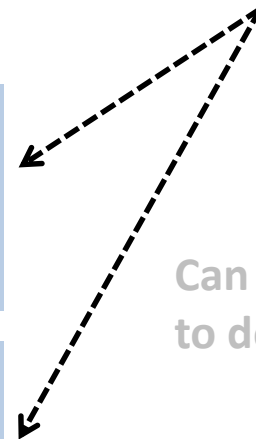


Treatment planning :

- Surgery (Extent of resection)
- Radiotherapy (Segmentation, Dose)
- Systemic therapy

Clinical outcome :

- Final diagnosis
- Response to therapy (prediction)
- Prognosis (DFS, OS)



Can be used
to determine

Radiomics

Applications for Neuro-Oncology

- **Prediction of clinical outcome**
- **Non-invasive determination of molecular biomarkers**
- **Tumor segmentation**
- **Differentiation of recurrence from radionecrosis**

Radiomics based on Feature Description: Typical Workflow

- 1) Manual segmentation of tumor (and compartments)
- 2) Preprocessing (filterung etc.)
- 3) Feature computation/ extraction
- 4) Model building (classification) using clinical or genomic data
- 5) Validation of the model using independent data set

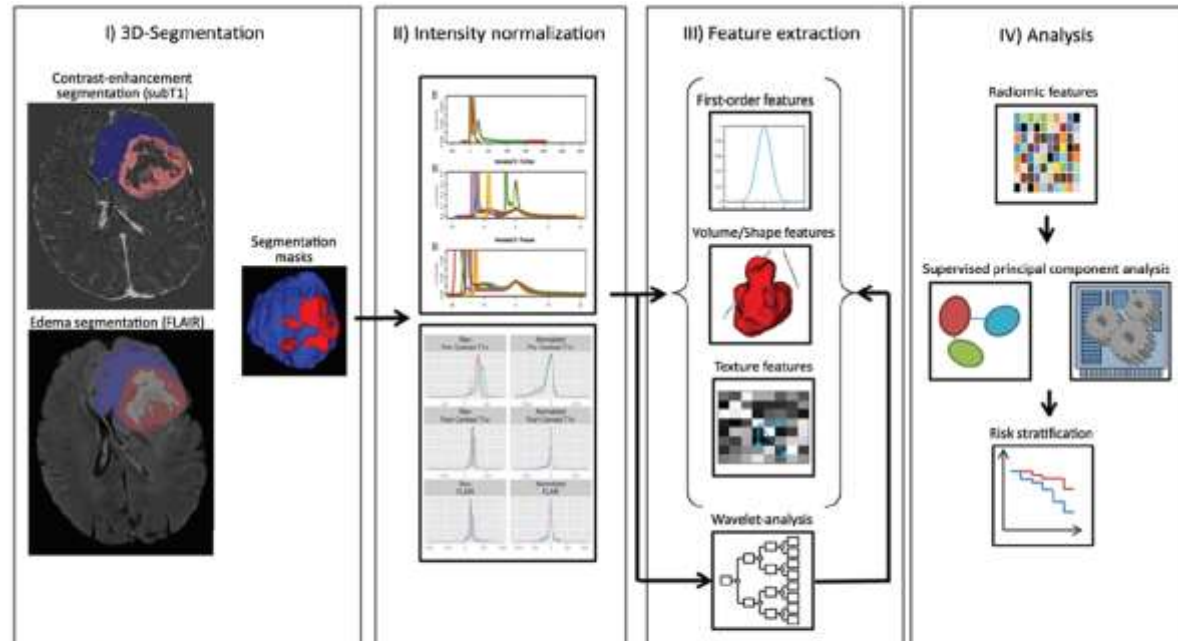


Figure 1: Image postprocessing workflow is shown. Tumors have different shapes and levels of intensity, as shown on representative images. On left images, tumor segmentations are red, with the volume-rendered three-dimensional (3D) segmentations on the right. Workflow from tumor segmentation to statistical analysis is shown in order (left to right). *I* = Segmentation of contrast-enhancing (red mask) and nonenhancing (blue mask) tumor volume on coregistered, brain-extracted T1-weighted subtraction (subT1) and FLAIR volume images. *II* = Image intensity levels are normalized into common parameter space that allows referencing among different subjects. *III* = Multiple radiomic features are automatically calculated from intensity-normalized contrast-enhanced T1-weighted and FLAIR volume images by using three-dimensional segmentations including first-order, volume and shape, and texture features. In addition, three-dimensional wavelet decomposition is performed on original images and decomposed images subjected to the same feature extraction routine. *IV* = Large number of radiomic feature parameters is then subjected to SPCA analysis for determination of suitable parameters for survival stratification.

Radiomics: Feature extraction and Model building using CNN (Convolutional Neural Networks)

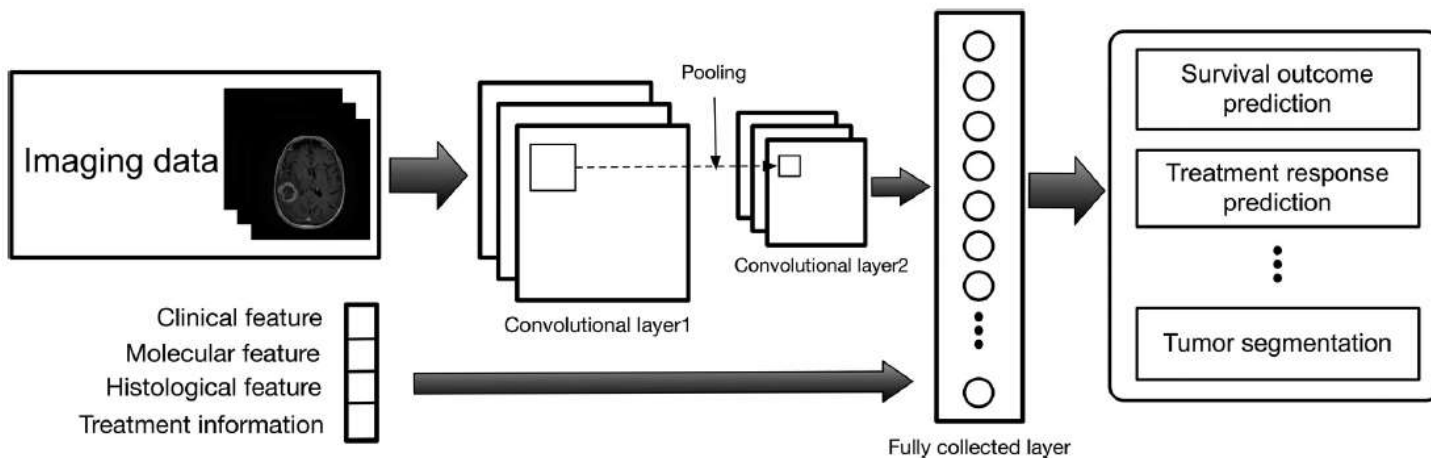
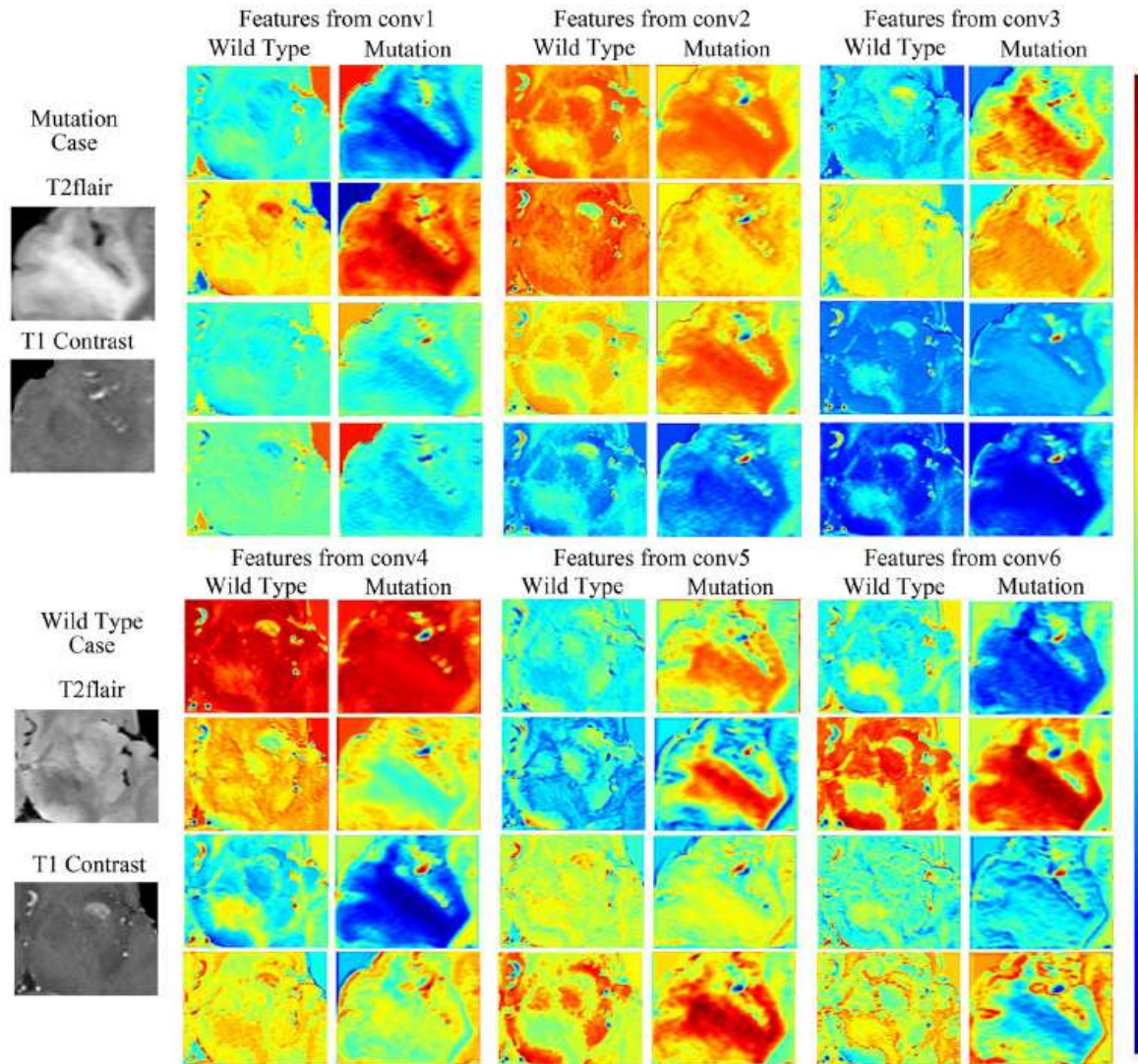


FIG 3. Illustration of the convolutional neural networks model using imaging and other biomedical data for brain tumor analysis. The convolutional neural networks model consists of multiple convolutional layers, pooling layers, and fully connected layers to learn an abstraction of the input data, such as imaging and clinical features for a variety of outcome evaluations.

Radiomics in Brain Tumor: Image Assessment, Quantitative Feature Descriptors, and Machine-Learning Approaches

M. Zhou, J. Scott, B. Chaudhury, L. Hall, D. Goldgof, K.W. Yeom, M. Iv, Y. Ou, J. Kalpathy-Cramer, S. Napel, R. Gillies, O. Gevaert, and R. Gatenby

Radiomics: Feature Maps



Deep Learning based Radiomics (DLR) and its usage in noninvasive IDH1 prediction for low grade glioma

Zejun Li¹, Yuan Yuan Wang^{1,2}, Jinhua Yu^{1,2}, Yi Guo^{1,2}, Wei Cao¹

SCIENTIFIC REPORTS | 7: 5467

Figure 4. Feature maps of CNN features from different convolutional layers. The four most significant filter banks of different layers were selected. As shown in the figures, feature maps of deeper layers represented more detailed characteristics.

Radiomics for Survival prediction in GBM based on tumor region

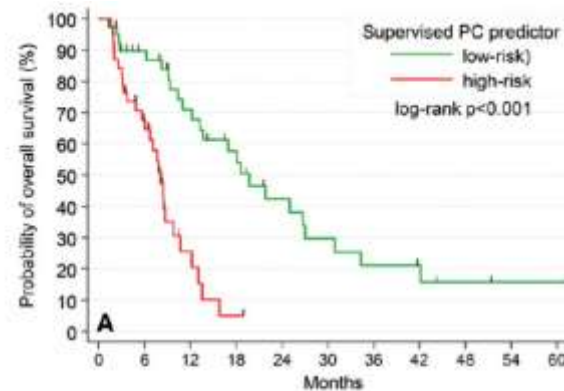
Radiomic Profiling of

Glioblastoma: Identifying an Imaging Predictor of Patient Survival with Improved Performance over Established Clinical and Radiologic Risk Models¹

Radiology: Volume 280: Number 3—September 2016

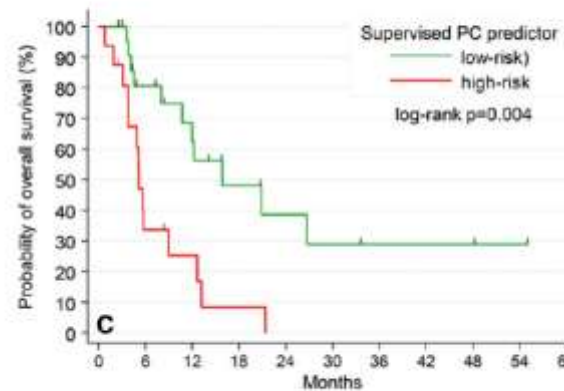
Philipp Kickingereder, MD

- **11 significant features selected from a set of ca. 12000**
- **All 11 features from FLAIR signal of the contrast enhancing regio**
- **Most significant feature related to tumor heterogeneity**



training

Number at risk	0	6	12	18	24	30	36	42	48	54	60
low-risk	40	31	22	16	10	7	5	4	2	1	1
high-risk	39	22	5	1	0	0	0	0	0	0	0



validation

Number at risk	0	6	12	18	24	30	36	42	48	54	60
low-risk	24	15	10	6	4	3	2	2	2	1	0
high-risk	16	5	3	1	0	0	0	0	0	0	0

Radiomics for Survival prediction in GBM: based on peritumoral parenchyma

Radiomic features from the peritumoral brain parenchyma on treatment-naïve multi-parametric MR imaging predict long versus short-term survival in glioblastoma multiforme: Preliminary findings

Eur Radiol (2017) 27:4188–4197

Prateek Prasanna¹ · Jay Patel¹ · Sasan Partovi² · Anant Madabhushi¹ · Pallavi Tiwari¹ 

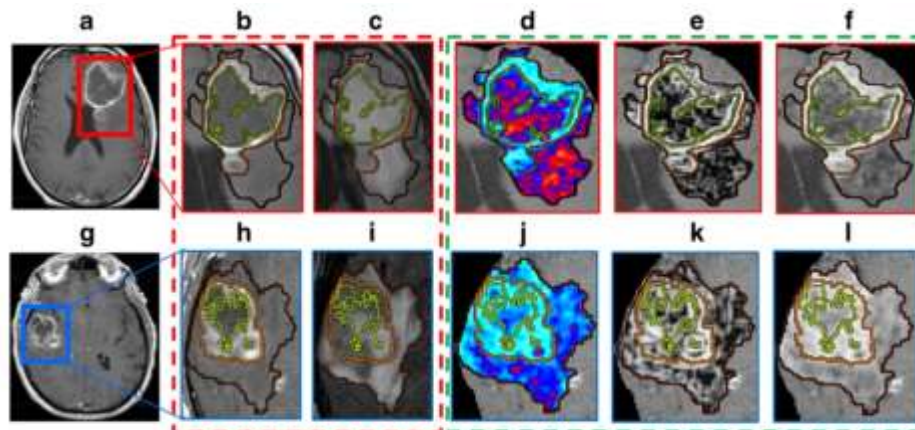
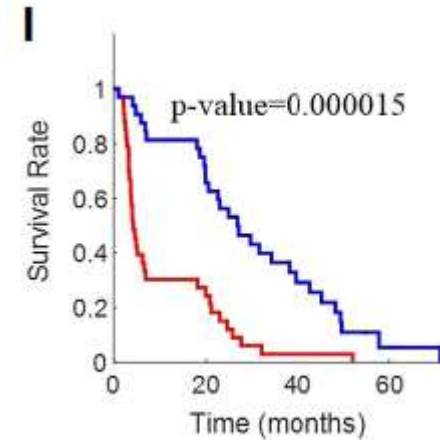
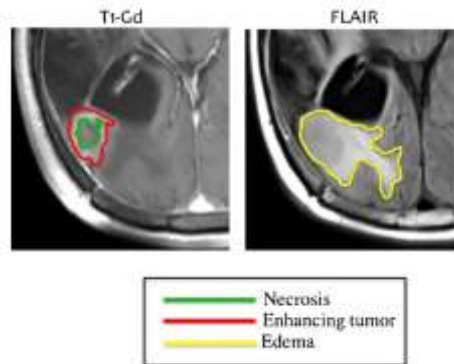


Fig. 3 A single two-dimensional gadolinium (Gd)-T_{1w} MRI slice for two different patients with short- (a) and long- (g) term survival, respectively. The expert-annotated region bounded in green is necrosis; the region bounded in orange is enhancing tumour, while the region bounded in

black is oedema. The corresponding per-voxel representations of three Haralick descriptors are shown for entropy (d, j), Correlation (e, k), and Sum Entropy (f, l) features

Table 4 Five of the most predictive radiomic features from peritumoral brain zone (PBZ) across the three magnetic resonance (MR) sequences gadolinium (Gd)contrast T_{1w}, T_{2w} and FLAIR, as well as across the multi-parametric set. Note that W5W5 represents a laws feature that captures wave patterns in an image using a 5 × 5 filter. Similarly, R5R5 represents a laws feature that captures ripple patterns, S5S5 captures spot patterns, while E5E5 captures the edge patterns in an image

T _{1w}	T _{2w}	FLAIR	Multi-parametric MRI
W5W5	E5E5	W5W5	R5R5 (T _{1w})
R5R5	R5R5	R5R5	Sum variance (T _{1w})
Sum variance	W5W5	S5S5	R5R5 (T _{2w})
E5E5	S5S5	E5E5	E5E5 (T _{2w})
L5L5	Correlation	L5L5	R5R5 (FLAIR)

Radiomics for survival prediction in GBM: Results

Author	N train. /valid.	MRI methods	Primary feature set	Selection method	Final feature set	Classification method	Tumor subregions	Prediction accuracy (valid. set if available)
Lee (2015)	65 / 0	T1-CE, FLAIR	36 (habitats)	CoV	5	Symbolic Regression	all subregions	p = 0.00021 OS </> 12 m
McGarry (2016)	81 / 0	T1/CE, DWI, FLAIR	81 (intensity)	Kaplan-Maier/ log rank test	5	Score (vol. threshold)	CE-region (T1-CE)	p < 0.005 median OS 25m vs. 8m
Kickingeder (2016)	79 / 40	T1/CE, DWI, FLAIR	12190	Supervised PCA	11	Radiomics Score	CE-region (FLAIR)	p < 0.004 HR 3.45
Prasanna (2017)	65 / 0	T1-CE, T2, FLAIR	3x 402	mRMR	10	Random Forest	peritumoral	p < 0.0001 OS < 7m vs. > 18m
Lao (2017)	75 / 37	T1/CE, T2, FLAIR	98304	CNN-S, C-Index, LASSO	6	Score (linear comb.)	mainly tumor core	p < 0.001 HR = 5.13
Li (2017)	60 / 32	T1/CE, T2, FLAIR	45792	OCCC, C-index, LASSO	4	Score	all subregions	p < 0.004 HR = 3.29

Abrevatations:

PCA: Principal Component Analysis

mRMR: minimum Redundancy Maximum Relevance

CoV: Coefficient of Variation

CNN: Convolutional Neural Network

ROC: Receiver Operator Characteristics

SVM: Support Vector Machine

OCCC: Overall Concordance Correlation Coefficient

Radiomics for prediction of IDH1 mutation in glioma

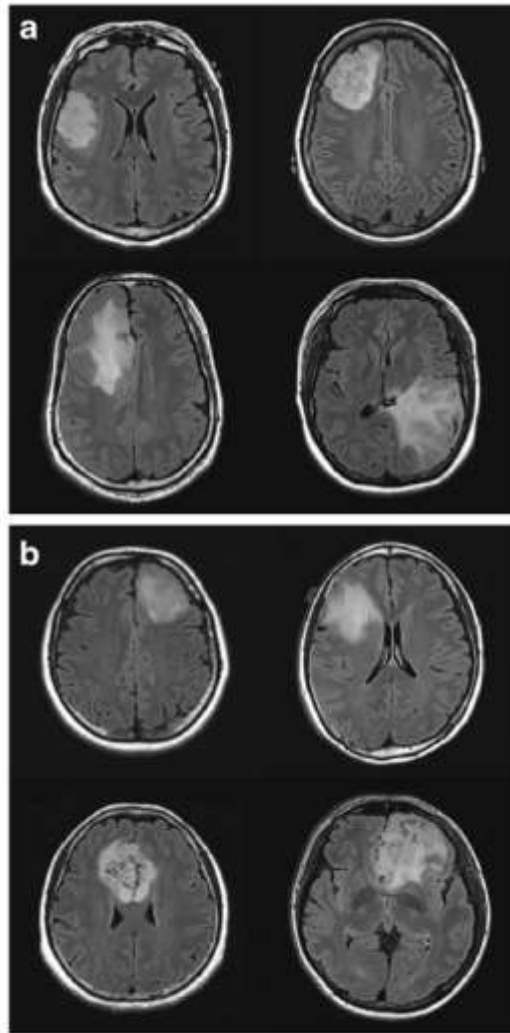
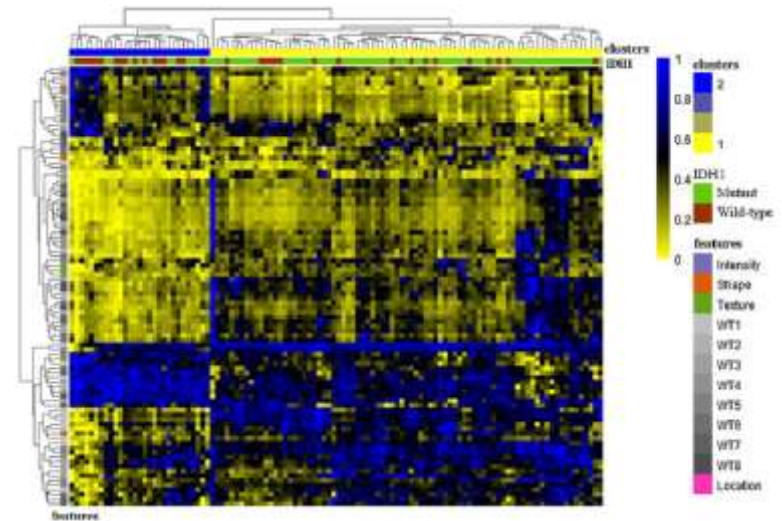


Fig. 4 Representative cases to show shape and texture differences between different isocitrate dehydrogenase 1 (IDH1) states. (a) Representative shapes, (b) representative texture features. First row of (a) and (b): two typical cases in an IDH1 mutation group; second row of (a) and (b): two typical cases in a wild-type group

Noninvasive IDH1 mutation estimation based on a quantitative radiomics approach for grade II glioma

Jinhua Yu^{1,2} · Zhifeng Shi² · Yixi Lian¹ · Zeju Li¹ · Tongtong Liu¹ · Yuan Gao² · Yuanyuan Wang¹ · Liang Chen² · Ying Mao²

Eur Radiol (2017) 27:3509–3522



	Classifier	Feature number	AUC
Primary cohort (110 cases)	SVM	671	0.76
		197	0.84
		110	0.86
	AdaBoost	671	0.68
		197	0.77
		110	0.81
Validation Cohort (30 cases)	SVM	110	0.79
	AdaBoost	110	0.80

MR radiomics for determination of IDH1/2 mutations in glioma

Author	Tumor type Biomarker	MRI methods	N train/valid	Primary feature set	Selection method	Final feature set	Classification method	Diagnostic accuracy (valid. Set if available)
Zhou (2017)	WHO II IDH mut / wt 75% / 25%	T1/CE, T2, FLAIR	165 / 0	4x 42	ROC	3	Multivariate Logistic regression	77% (estim.)
Yu (2016)	WHO II IDH mut / wt 71% / 29%	FLAIR	110 / 30	671	mRMR	110	SVM	83%
Li (2017)	WHO II IDH mut / wt 74% / 26%	T1/CE, FLAIR	60 / 59	16384	CNN (segm.) Fisher vector t-test, F-score	494	SVM	91%
Eichinger (2017)	WHO II/III IDH mut / wt 75% / 25%	T2, DTI	59 / 20	101 (LBP)	none	101	Neural Network (single layer)	95%
Zhang (2017)	WHO III/IV IDH mut / wt 45% / 55%	T1/CE, T2, FLAIR, DWI	90 / 30	2970	ROC, Redundancy reduction	386	Random Forest	89%

Abrevatations:

mRMR: minimum Redundancy Maximum Relevance

CNN: Convolutional Neural Network

ROC: Receiver Operator Characteristics

SVM: Support Vector Machine

LBP: Local Binary Patterns

MR radiomics for determination of MGMT and 1p/19q-Status in glioma

Author	Tumor type Biomarker	MRI methods	N train /valid	Feature Set	Selection method	Final features	Classification method	Diagnostic accuracy (valid. set if available)
Korfiatis (2016)	GBM MGMT methyl /non 43% / 57%	T1/CE, T2	155 / 0	18	Ridge regressio n	4	SVM Random Forest	81%
Xi (2016)	GBM MGMT methyl /non 44% / 56%	T1/CE, T2	98 / 20	1665	LASSO	36	SVM	80%
Han (2018)	GBM MGMT methyl /non n.a.	T1, T2, FLAIR	117 / 42	512 (nodes in final layer)	CRNN L2-regul.	n.a.	Softmax	62%
Zhou (2017)	WHO II 1p/19q codel / non 25% / 75%	T1/CE, T2, FLAIR	165 / 0	4x 42	ROC	3	Multivariate Log. Regress.	90%
Shofty (2017)	WHO II 1p/19q codel / non 55% / 45%	T1CE, T2, FLAIR	47 / 0	152	MWU- test PCA	9	Ensemble Bagged Trees	87%

Abrevatations:

CRNN: Convolutional Recurrent Neural Network

CNN: Convolutional Neural Network

ROC: Receiver Operator Characteristics

SVM: Support Vector Machine

MWU: Mann-Whitney U-test

PCA: Principle Component Analysis

Radiomics

Tumor Segmentation

The Multimodal Brain Tumor Image Segmentation Benchmark (BRATS)

IEEE TRANSACTIONS ON MEDICAL IMAGING, VOL. 34, NO. 10, OCTOBER 2015

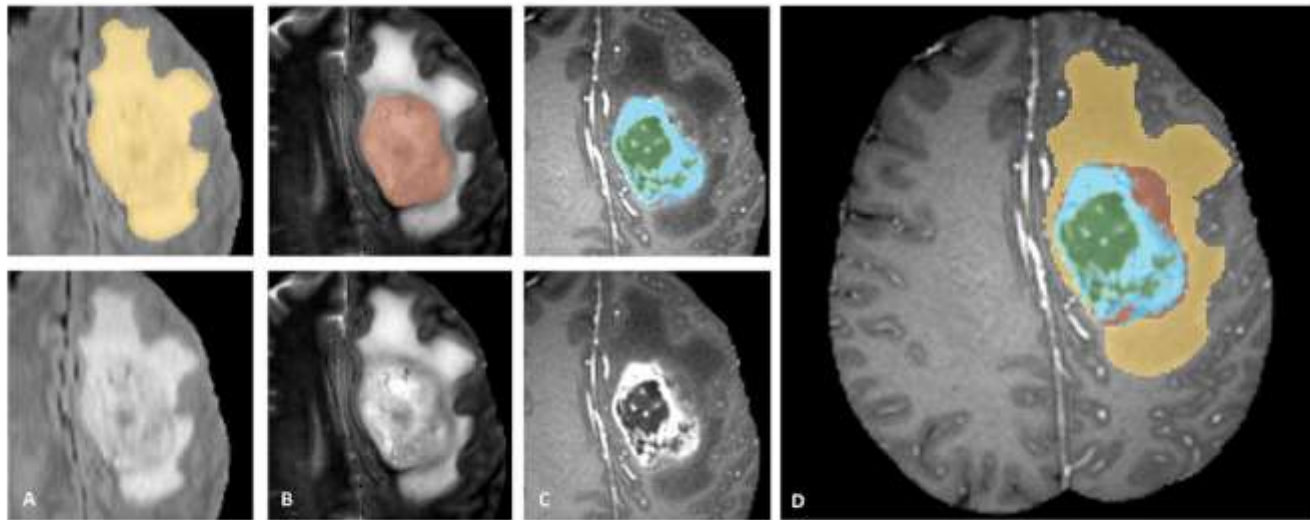


Fig. 3. Manual annotation through expert raters. Shown are image patches with the tumor structures that are annotated in the different modalities (top left) and the final labels for the whole dataset (right). Image patches show from left to right: the *whole* tumor visible in FLAIR (A), the tumor *core* visible in T2 (B), the *enhancing* tumor structures visible in T1c (blue), surrounding the *cystic/necrotic components* of the core (green) (C). Segmentations are combined to generate the final labels of the tumor structures (D): edema (yellow), non-enhancing solid core (red), necrotic/cystic core (green), enhancing core (blue).

Radiomics: Segmentation

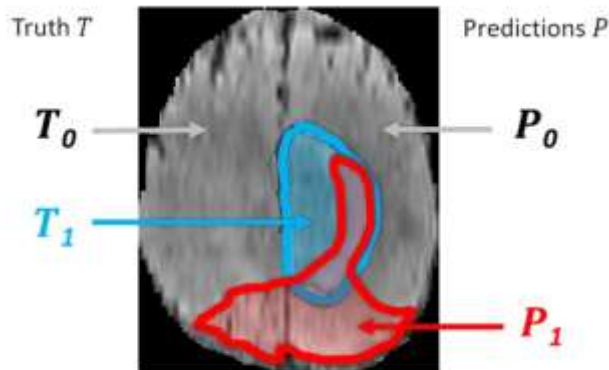


Fig. 4. Regions used for calculating Dice score, sensitivity, specificity, and robust Hausdorff score. Region T_1 is the true lesion area (outline blue), T_0 is the remaining normal area. P_1 is the area that is predicted to be lesion by—for example—an algorithm (outlined red), and P_0 is predicted to be normal. P_1 has some overlap with T_1 in the right lateral part of the lesion, corresponding to the area referred to as $P_1 \wedge T_1$ in the definition of the Dice score (Eq. III.E).

The Multimodal Brain Tumor Image Segmentation Benchmark (BRATS)

IEEE TRANSACTIONS ON MEDICAL IMAGING, VOL. 34, NO. 10, OCTOBER 2015

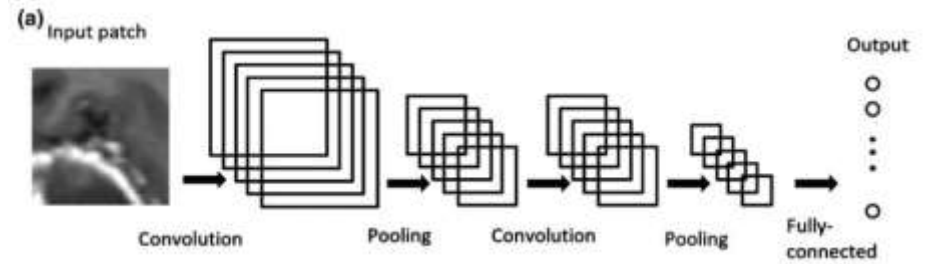
$$\text{Dice}(P, T) = \frac{|P_1 \wedge T_1|}{(|P_1| + |T_1|)/2}$$

■ Buendia	Bit-grouping artificial immune network
■ Cordier	Patch-based tissue segmentation approach
■ Doyle	Hidden Markov fields and variational EM in a generative model
■ Festa	Random forest classifier using neighborhood and local context features
■ Guo	Semi-automatic segmentation using active contours
■ Meier	Appearance- and context-sensitive features with a random forest and CRF
■ Reza	Texture features and random forests
■ Taylor	“Map-Reduce Enabled” hidden Markov models
■ Tustison	Random forest classifier using the open source ANTs/ANTsR packages
■ Zhao (II)	Like “Zhao (I)” with updated unary potential

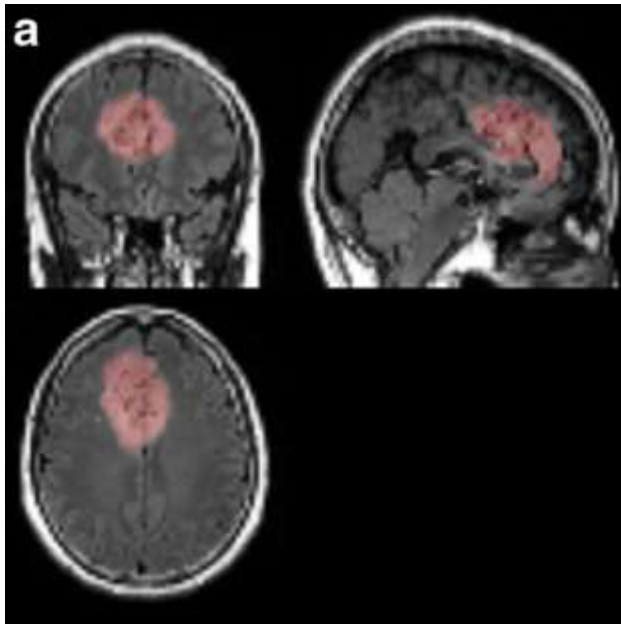
BRATS 2013			
Real data	whole	core	active
Dice (in %)	<i>HG only</i>	<i>HG only</i>	
■ Cordier	84	68	65
■ Doyle	71	46	52
■ Festa	72	66	67
■ Meier	82	73	69
■ Reza	83	72	72
■ Tustison	<u>87</u>	<u>78</u>	<u>74</u>
■ Zhao (II)	84	70	65

Radiomics

CNN for tumor segmentation

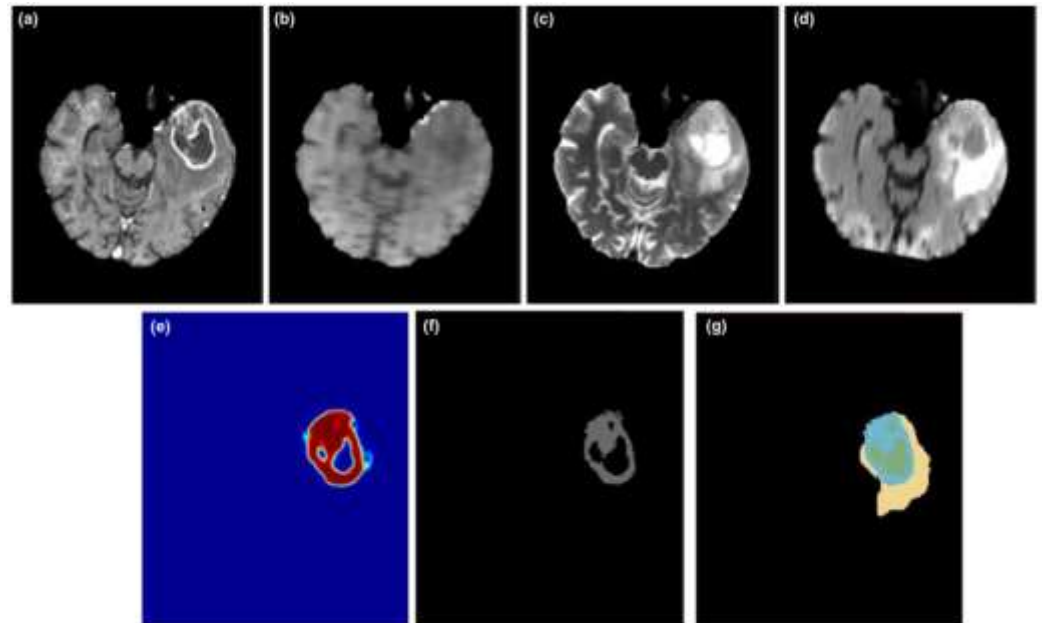


Low grade glioma



Yu J, Eur Radiol 2017

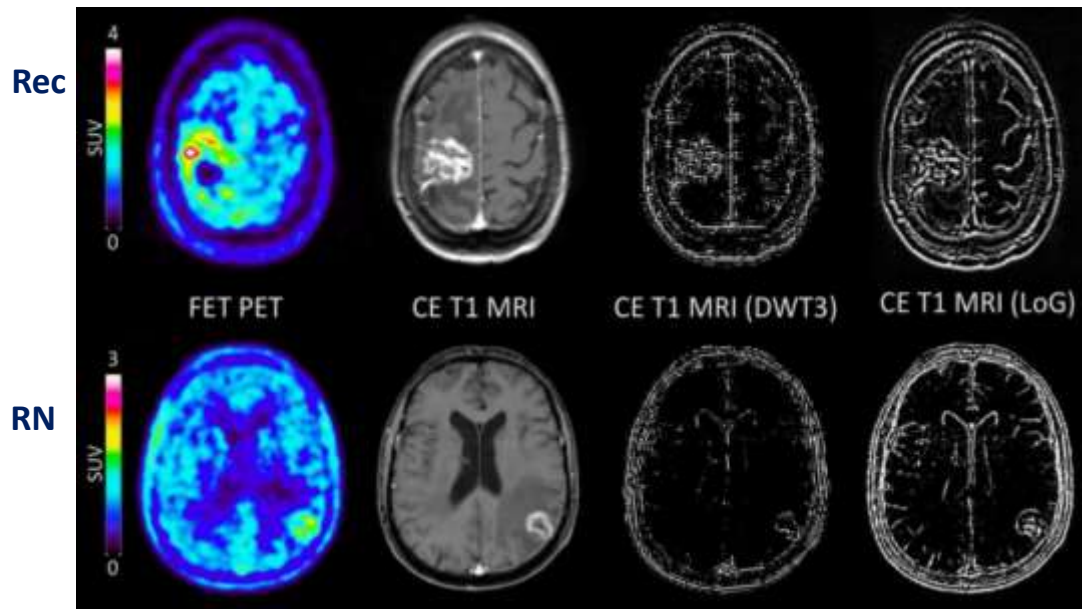
High grade glioma



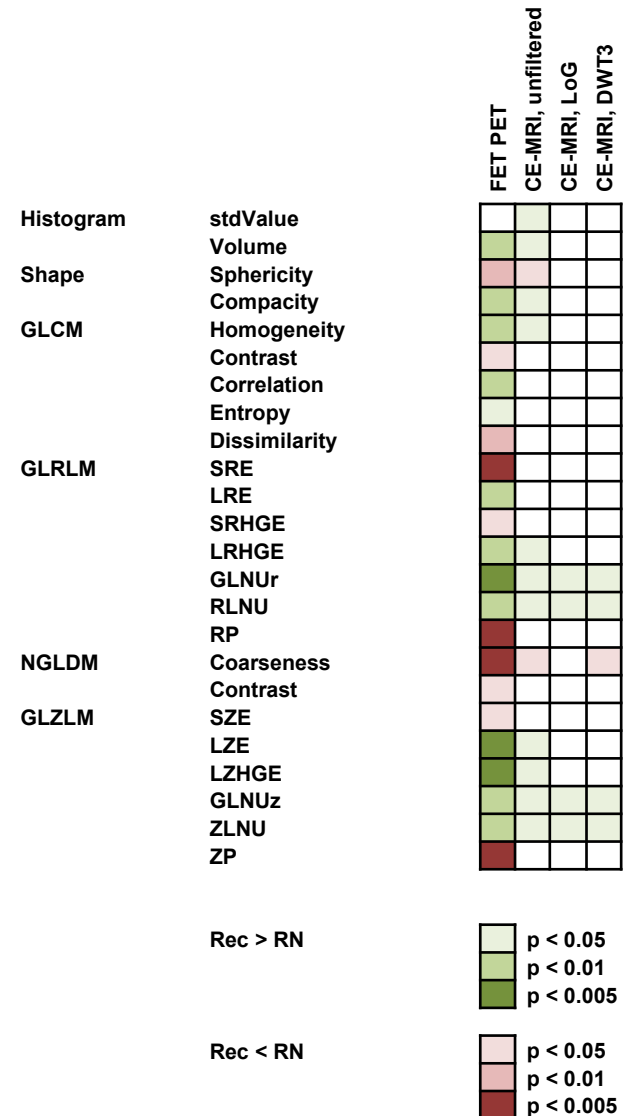
Zhuge J, MedPhys 2017

Combined FET-PET/MRI Radiomics

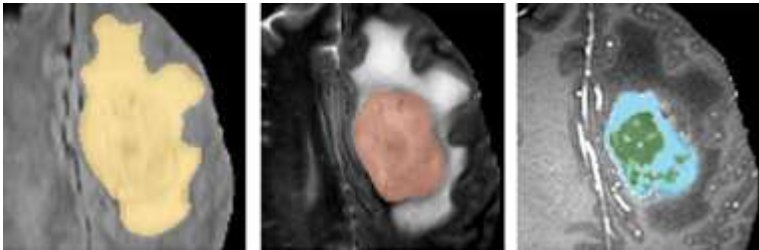
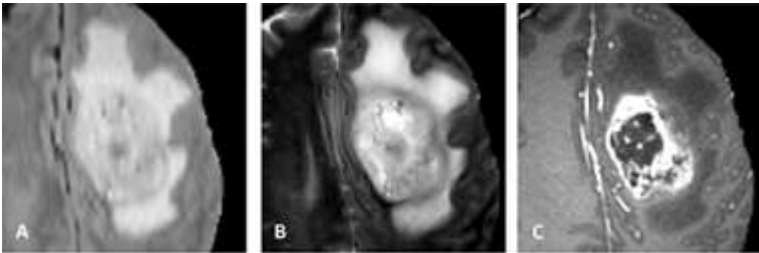
Discrimination of radiation necrosis from recurrence in metastases treated by radiosurgery



	<u>accuracy</u>
MRI	81%
FET-PET	83%
Combined	89%



Hi, this is *NeuroCast^R*, your personal digital assistant in Neuro-Oncology, please enter images:



... segmentation
... computing features
... generating predictions

Probability GBM: 90%
Probability AA: 5%
Probability OD: 0%

Probability IDH-mut: 37%
Probability 1p/19q code1: 1%
Probability MGMT-methyl: 56%

Prediction Survival@1year: 48%

... generating resection mask

Radiomics: Summary

- Digital images contain a large amount of data
- Methods from digital image processing & statistics
- Convolutional neural networks

- Outcome prediction from radiomic features
- Assessment of genetic markers (accuracy 80-90%)
- Visualisation of feature maps
- Advanced methods for tumor segmentation